# Breakdown of the Independent Particle Approximation in High-Energy Photoionization

E. W. B. Dias, H. S. Chakraborty, and P. C. Deshmukh
*Department of Physics, Indian Institute of Technology—Madras, Madras 600036, India*

Steven T. Manson
*Department of Physics and Astronomy, Georgia State University, Atlanta, Georgia 30303*

O. Hemmers, P. Glans, D. L. Hansen, H. Wang, S. B. Whitfield, and D. W. Lindle
*Department of Chemistry, University of Nevada, Las Vegas, Nevada 89154-4003*

R. Wehlitz, J. C. Levin, and I. A. Sellin
*Department of Physics and Astronomy, University of Tennessee, Knoxville, Tennessee 37996-1200*

R. C. C. Perera
*Advanced Light Source, Lawrence Berkeley Laboratory, Berkeley, California 94720*
(Received 18 February 1997)

The independent particle approximation is shown to break down for the photoionization of both inner and outer $n\ell$ ($\ell > 0$) electrons of all atoms, at high enough energy, owing to interchannel interactions with the nearby $ns$ photoionization channels. The effect is illustrated for Ne $2p$ in the 1 keV photon energy range through a comparison of theory and experiment. The implications for x-ray photoelectron spectroscopy of molecules and condensed matter are discussed. [S0031-9007(97)03382-6]

PACS numbers: 32.80.Fb

The response of physical systems to ionizing electromagnetic radiation, photoionization, is a basic process of nature. Because of the weak coupling between incident photons and target electrons, the electromagnetic radiation exerts only a small perturbation on the target, thereby allowing the unambiguous study of target electron properties, e.g., correlation and many-body aspects of electron dynamics. In addition, the photoionization process, along with associated spectroscopies including photoelectron spectroscopy, is of importance in a variety of applications [1] including structural determination in crystalline solids, astrophysical modeling, radiation physics, etc. Owing to its importance, the field has seen a recent upsurge of activity, particularly in the x-ray range, due to the development of third generation synchrotron radiation sources on the experimental side [2], along with the dramatic increase in computer power available, on the theoretical side.

In recent years, a wide variety of studies, both theoretical and experimental, have shown the importance of correlation in the form of interchannel coupling on the photoionization process in the region of the outer shell thresholds [3–10]; in some cases, the single-particle viewpoint breaks down completely. An outstanding example is the threshold behavior of Xe $5s$ which is completely dominated by interchannel coupling with the $5p$ and $4d$ channels [5]. In addition, in the vicinity of inner shell thresholds, dramatic effects are seen in outer shell cross sections due to interchannel coupling. Examples of this phenomenon abound [7], e.g., effects on the outer shell cross sections of atomic Ba in the vicinity of the $4d$ threshold [11]. It is generally thought, however, that in the x-ray range (far from the first ionization potential) away from inner shell ionization thresholds, the photoionization process can be well characterized in a single channel [3,7,12,13], or independent particle approximation, theory which omits correlation entirely. If this assertion is not true, then doubt is cast upon the interpretation of a number of studies of atoms, molecules, and condensed matter involving x-ray photoabsorption.

In this paper it is shown that this notion is *not* true for the photoionization of *any* $n\ell$ ($\ell > 0$) subshell at high enough energy, but is true for $ns$ subshell photoionization. To understand why this occurs, we first scrutinize the basic idea of interchannel coupling in some detail. Consider a simple situation where, within the framework of an independent particle theory (such as Hartree-Fock), the ground state of the target system is characterized by $\psi_i$ and there are two final channels with wave functions $\psi_{1,\varepsilon}$ and $\psi_{2,\varepsilon}$ with $\varepsilon$ the total energy; all of these wave functions being eigenfunctions of $H_0$, an approximation to the exact Hamiltonian of the system, $H$. For simplicity, we shall assume that there is no *intrachannel* coupling, i.e.,

$$\langle \psi_{j,\varepsilon} | H | \psi_{j,\varepsilon'} \rangle = \varepsilon \delta(\varepsilon - \varepsilon'), \tag{1}$$

which is a property of a Hartree-Fock theory [14]. Now, consider a transition process under the action of transition operator $T$, and define the transition matrix elements

$$D_j(\varepsilon) = \langle \psi_i | T | \psi_{j,\varepsilon} \rangle, \qquad j = 1, 2. \tag{2}$$

The "real" wave functions for the final states, the eigenfunctions of $H$, can be constructed as linear combinations

  

of the $\psi_{1,\varepsilon}$'s and the $\psi_{2,\varepsilon}$'s. Using first order perturbation theory to approximate the "exact" wave functions, as modified to deal with the continuum [14], we obtain for the corrected wave functions

$$\Psi_{1,E} = \psi_{1,E} + P\int \frac{\langle\psi_{2,\varepsilon}|H - H_0|\psi_{1,E}\rangle}{E - \varepsilon}\,\psi_{2,\varepsilon}\,d\varepsilon\,, \quad (3a)$$

$$\Psi_{2,E} = \psi_{2,E} + P\int \frac{\langle\psi_{1,\varepsilon}|H - H_0\psi_{2,E}\rangle}{E - \varepsilon}\,\psi_{1,\varepsilon}\,d\varepsilon\,, \quad (3b)$$

where $P$ represents the principal value. The perturbed matrix elements then become

$$M_1(E) = D_1(E) + P\int \frac{\langle\psi_{2,\varepsilon}|H - H_0|\psi_{1,E}\rangle}{E - \varepsilon}\,D_2(\varepsilon)\,d\varepsilon\,, \quad (4a)$$

$$M_2(E) = D_2(E) + P\int \frac{\langle\psi_{1,\varepsilon}|H - H_0|\psi_{2,E}\rangle}{E - \varepsilon}\,D_1(\varepsilon)\,d\varepsilon\,. \quad (4b)$$

These equations embody the notion of interchannel coupling, i.e., the transition matrix element of each channel being modified owing to the fact that the real wave functions of the system involve a mixture of channels. For example, for electric dipole photoionization of Xe $5s$, let channel 1 be $5s \rightarrow kp$ and channel 2, $5p \rightarrow kd$. Equation (4a) then becomes

$$M_{5s\rightarrow kp}(E) = D_{5s\rightarrow kp}(E) + P\int \frac{\langle\psi_{5p\rightarrow k'd}|H - H_0|\psi_{5s\rightarrow kp}\rangle}{E - \varepsilon} \times D_{5p\rightarrow k'd}(\varepsilon)\,d\varepsilon\,. \quad (5)$$

Because these channels are degenerate, the denominator, $E - \varepsilon$, can vanish. Further, the interaction matrix element in the numerator of Eq. (5), essentially a matrix element of $e^2/r_{ij}$, is not small. Thus, since $D_{5p\rightarrow kd}$ is much larger than $D_{5s\rightarrow kp}$, the integral term in Eq. (5) dominates the matrix element over a broad range above the $5s$ ionization threshold. Significant effects attributable to this behavior are confirmed by experiment [5].

Similarly, in the photoionization of Ba $6s$ around the $4d$ threshold, the dipole matrix element becomes

$$M_{6s\rightarrow kp}(E) = D_{6s\rightarrow kp}(E) + P\int \frac{\langle\psi_{4d\rightarrow k'f}|H - H_0|\psi_{6s\rightarrow kp}\rangle}{E - \varepsilon} \times D_{4d\rightarrow k'f}(\varepsilon)\,d\varepsilon \quad (6)$$

and the second term dominates, just like Xe $5s$, because $D_{4d\rightarrow kf}$ is much larger than $D_{6s\rightarrow kp}$. There is, however, a difference in the two cases. In the latter case, the second term dominates only in a limited range around the $4d$ threshold. For energies below the threshold, the second term falls off rapidly due to the energy denominator. Above the threshold, it falls off because the interaction matrix element decreases with increasing energy as a result of the destructive interference between the continuum waves of the two channels which have rather different energy for a given $h\nu$. Only near the $4d$ threshold, where the $kf$ wave function is not very oscillatory, is the interaction matrix element large. In the Xe $5s$ case, by contrast, because the $5s$ and $5p$ have roughly the same binding energy, the continuum waves remain roughly "in phase" at all energies so that the interaction matrix element falls off only very slowly with energy and the interchannel coupling effects persist over a large energy range.

Now, consider the photoionization of an $np$ electron, inner or outer, from any atom, molecule, or solid. Not far above the $np$ ionization threshold will always be an $ns$ threshold. Thus, a bit above the $np$ threshold, there will always be an $ns$ cross section degenerate with the $np$ cross section. However, no matter what the relative values of these cross sections are near the thresholds, at energies far above threshold the $ns$ cross section will *always* dominate the $np$. This is because, at high energy, the electric dipole photoionization cross section for an $n\ell$ subshell falls off with energy as $E^{-(7/2+\ell)}$ [3,7]. Thus, using Eqs. (4),

$$M_{np\rightarrow kd(s)}(E) = D_{np\rightarrow kd(s)}(E) + P\int \frac{\langle\psi_{ns\rightarrow k'p}|H - H_0|\psi_{np\rightarrow kd(s)}\rangle}{E - \varepsilon} \times D_{ns\rightarrow k'p}(\varepsilon)\,d\varepsilon\,. \quad (7)$$

Because the energies of the photoelectrons from the $np$ and $ns$ channels are similar, the interaction matrix element falls off only very slowly and remains large with increasing energy, much like the Xe $5s$ case. Thus, for both $np \rightarrow kd$ and $np \rightarrow ks$, the second term in Eq. (7) becomes a larger and large contribution to the matrix element, with increasing energy. This is in sharp contradistinction to the notion that the single-particle characteristics of the electric dipole photoionization process dominate at high energy.

As a prototypical example, consider the photoionization of atomic Ne in the 1 keV photon energy range. Calculations were performed within the framework of the relativistic random-phase approximation (RRPA) [15,16] for the cross section, $\sigma$, and photoelectron angular distribution asymmetry parameter, $\beta$, of the $2p$ subshell. Four levels of approximation were considered: (i) coupling of all of the relativistic single excitation channels arising from $2p$, $2s$, and $1s$; (ii) from $2p$ and $2s$ only; (iii) from $2p$ and $1s$ only; and (iv) from $2p$ alone and $2s$ alone.

The results for the $2p$ partial cross section of Ne are shown in Figs. 1 and 2. From these results, it is seen that the calculation predicts that all four levels of calculation agree rather well at the lowest energies considered. This is because the $2p$ cross section dominates the $2s$ cross section in this energy range by a factor of about 6, so that interchannel coupling does not appreciably affect

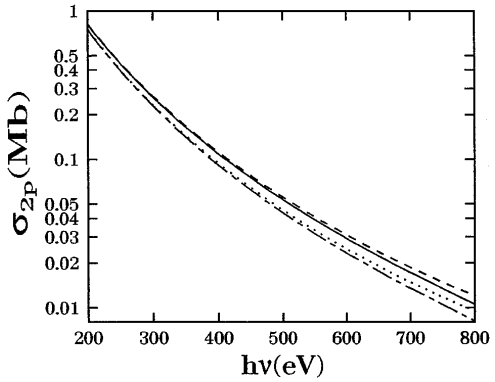


FIG. 1. Photoionization cross section for Ne $2p$ between 200 and 800 eV. The curves are RRPA results with the single excitation channels arising from $2p$, $2s$, and $1s$ coupled (solid curve); $2p$ and $2s$ (dashed curve); $2p$ and $1s$ (dash-dotted curve); and $2p$ alone (dotted curve).

the $2p$ matrix elements. With increasing photon energy, however, the $2p$ matrix elements fall off more rapidly than the $2s$, so that by the 500 eV range, the $2s$ cross section is larger than the $2p_{3/2}$ by a factor of 2 and larger than the $2p_{1/2}$ by a factor of more than 3. This translates into two groups of results in this energy range as seen in Fig. 1. The two calculations with $2p$ and $2s$ coupled agree with each other, and the other two agree with each other but disagree with the first group. This clearly points to the interchannel coupling between $2p$ and $2s$ channels being responsible for this difference. With increasing energy, this behavior is interrupted as we approach 870 eV where the $1s$ channels open and coupling with them becomes crucial, as seen in Figs. 1 and 2. Above 1000 eV, however, we are back to the same two groups of curves, just as in the 500 eV region, indicating that in this region as well, it is the coupling of the $2p$ with the $2s$ channels that matters. The coupling produces a $2p$ cross section more than 30% above the uncoupled result, as seen in Fig. 2.

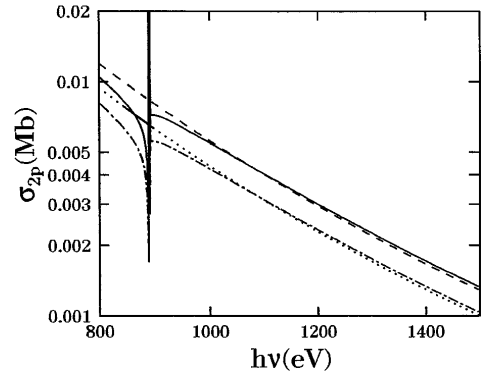


FIG. 2. Photoionization cross section for Ne $2p$ between 800 and 1500 eV. The curves are RRPA results with the single excitation channels arising from $2p$, $2s$, and $1s$ coupled (solid curve); $2p$ and $2s$ (dashed curve); $2p$ and $1s$ (dash-dotted curve); and $2p$ alone (dotted curve).

New measurements have been made for the ratio of the $2s$ to the $2p$ cross section, which take into account the nondipole contribution to the photoelectron angular distribution [17], and they are shown in Fig. 3, along with our theoretical results. These measurements confirm the accuracy by the excellence of the agreement. But the most important result demonstrated by Fig. 3 is the divergence between the fully coupled and the uncoupled calculations at the highest energies; and the fact that it is the coupling with $2s$ that is important as evidenced by the agreement between the full $(2p + 2s + 1s)$ calculation and the $2p + 2s$ calculation. In addition, a central field calculation [3,12,13] was performed using a Hartree-Slater potential [18] and the results (not shown) are virtually identical to the uncoupled $2p$ RRPA result of Fig. 3, as expected. Thus, it is clear that the single-particle result does not agree with experiment at the higher energies, while the coupled result does, in contrast to the conventional wisdom [3,7,12,13].

Looking at the photoelectron angular distribution parameter, $\beta$, the experimental results [17] along with the various levels of calculated results, are shown in Fig. 4; all levels of calculation agree reasonably well at the lowest energies, the separation into the same two groups occurs with increasing energy is seen, and the agreement of the experimental results with the full RRPA calculation is clear. Our single-particle result for $\beta$ (not shown) also is virtually indistinguishable from the $2p$ alone calculation. At the highest energies considered, we see about a 30% shift in $\beta$ from the single-particle calculation, reiterating the point that even out at 1.5 keV, approximately 100 times the threshold energy, interchannel coupling does matter.

This interchannel coupling effect should also be in evidence for $nd$ and $nf$ subshells as well, by the arguments

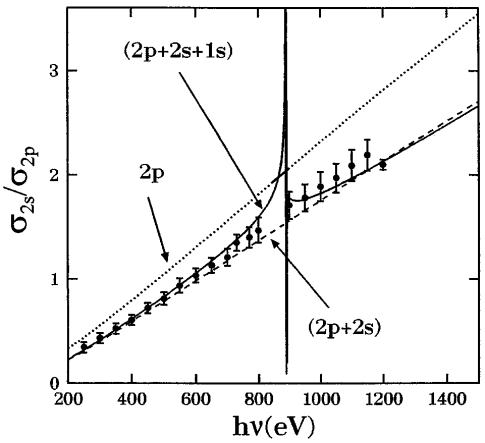


FIG. 3. Ratio of the $2s$ to $2p$ cross section for Ne. The calculations employed the RRPA formalism with the single excitation channels arising from $2p$, $2s$, and $1s$ coupled (solid curve); $2p$ and $2s$ coupled (dashed curve); and $2p$ and $2s$ *uncoupled* to each other (dotted curve). The experimental points were measured in the manner discussed in Ref. [17].

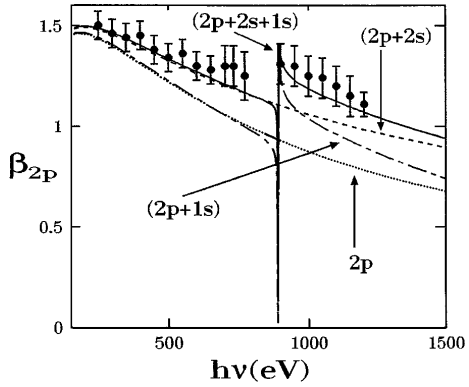


FIG. 4. Photoelectron angular distribution asymmetry parameter, $\beta$, for Ne $2p$ calculated using the RRPA formalism with the single excitation channels arising from $2p$, $2s$, and $1s$ coupled (solid curve); $2p$ and $2s$ (dashed curve); $2p$ and $1s$ (dash-dotted curve); and $2p$ alone (dotted curve). The experimental points are from Ref. [17] augmented by some new points reported here using the methodology of Ref. [17].

presented. In addition, although the detailed example was for an atom, the arguments are exactly the same for molecular and condensed matter targets. One *caveat* should be mentioned, however. At extremely high energies (tens of keV or higher), where relativistic interactions take over [19–21], the photoionization cross sections no longer behave as $E^{-(7/2+\ell)}$ and these arguments no longer apply. But for a very significant energy region below that, they do.

In conclusion, we have shown that the high-energy photoionization of all $n\ell$ ($\ell > 0$) subshells will exhibit a breakdown of the independent particle approximation owing to the effect of interchannel coupling with the nearby $ns$ channels, and this effect has been demonstrated for Ne $2p$ employing both theory and experiment. It is predicted that the same effect applies equally to molecules and condensed matter, as well as atoms.

This work was supported by the National Science Foundation, NASA, the Department of Energy, the Research Corporation, and the Petroleum Research Fund. The authors thank the staff of the ALS for their support and the IBM, LBNL, LLNL, University of Tennessee, and Tulane University Collaboration for beam time at beam line 8.0.

[1] *Applied Atomic Collision Physics*, edited by H. S. W. Massey, E. W. McDaniel, and B. Bederson (Academic Press, New York, 1983), 5 volumes.
[2] *New Directions in Research with Third Generation Soft X-Ray Sources*, edited by A. S. Schlachter and F. J. Wuilleumier, NATO ASI, Ser. E, (Kluwer, Dordrect, The Netherlands, 1992), Vol. 254.
[3] A. F. Starace, in *Handbuch der Physik*, edited by W. Mehlhorn (Springer-Verlag, Berlin, 1982), Vol. 31, pp. 1–121.
[4] J. A. R. Samson, in *Handbuch der Physik* (Ref. [3]), pp. 123–213.
[5] V. Schmidt, Rep. Prog. Phys. **55**, 1483 (1992).
[6] B. Sonntag and P. Zimmermann, Rep. Prog. Phys. **55**, 911 (1992).
[7] M. Ya. Amusia, *Atomic Photoeffect* (Plenum Press, New York, 1990).
[8] *Many-Body Theory of Atomic Structure and Photoionization*, edited by T.-N. Chang (World Scientific, Singapore, 1993).
[9] J. Berkowitz, *Photoabsorption, Photoionization, and Photoelectron Spectroscopy* (Academic Press, New York, 1979).
[10] H. P. Kelly, in *X-Ray and Inner-Shell Processes*, edited by T. A. Carlson, M. O. Krause, and S. T. Manson (American Institute of Physics, New York, 1990), pp. 292–314.
[11] J. M. Bizau, D. Cubaynes, P. Gerard, and F. J. Wuilleumier, Phys. Rev. A **40**, 3002 (1989).
[12] S. T. Manson and D. Dill, in *Electron Spectroscopy*, edited by C. R. Brundle and A. D. Baker (Academic Press, New York, 1978), Vol. 2, pp. 157–195.
[13] S. T. Manson, Adv. Electron. Electron Phys. **41**, 73 (1976).
[14] U. Fano, Phys. Rev. A **124**, 1866 (1961).
[15] W. R. Johnson and C. D. Lin, Phys. Rev. A **20**, 964 (1979).
[16] W. R. Johnson, C. D. Lin, K. T. Cheng, and C. M. Lee, Phys. Scr. **21**, 409 (1980).
[17] O. Hemmers, G. Fisher, P. Glans, D. L. Hansen, H. Wang, S. B. Whitfield, D. W. Lindle, R. Wehlitz, J. C. Levin, I. A. Sellin, R. C. C. Perera, E. W. B. Dias, H. S. Chakraborty, P. C. Deshmukh, and S. T. Manson (to be published).
[18] F. Herman and S. Skillman, *Atomic Structure Calculations* (Prentice-Hall, Englewood Cliffs, NJ, 1963).
[19] R. H. Pratt, A. Ron, and H. K. Tseng, Rev. Mod. Phys. **45**, 273 (1973).
[20] I. P. Grant, J. Phys. B **7**, 1458 (1974).
[21] A. Ron, I. B. Goldberg, J. Stein, S. T. Manson, R. H. Pratt, and R. Y. Yin, Phys. Rev. A **50**, 1312 (1994).